The Journal of Chemical Physics

Impact of cross-linking of polymers on transport of salt and water in polyelectrolyte membranes: A mesoscopic simulation study

Cite as: J. Chem. Phys. **149**, 224902 (2018); https://doi.org/10.1063/1.5057708
Submitted: 14 September 2018 . Accepted: 21 November 2018 . Published Online: 13 December 2018

Dipak Aryal, and Venkat Ganesan

Impact of cross-linking of polymers on transport of salt and water in polyelectrolyte membranes: A mesoscopic simulation study

Dipak Aryal and Venkat Ganesan[a)]
Department of Chemical Engineering, University of Texas at Austin, Austin, Texas 78712, USA

(Received 14 September 2018; accepted 21 November 2018; published online 13 December 2018)

Our recent atomistic simulation studies demonstrated that the transport properties of salt ions and water in non-crosslinked polymer electrolyte membrane exhibit an intriguing dependence on salt concentration that is opposite to that seen in electrolyte solutions. Here, we extend our study to probe the influence of the degree of cross-linking of the polymer on the transport properties of salt and water in polymer electrolyte membranes. Towards this objective, we use a coarse-grained model embedded within dissipative particle dynamics (DPD) mesoscale simulations, which allows us to access time scales necessary for studying crosslinked polymer systems. Our DPD simulations on non-crosslinked membranes reproduce results that are in qualitative agreement with our atomistic simulations. For the case of crosslinked membranes, our results demonstrate that the diffusion of salt ions and water is reduced significantly relative to crosslinked systems. However, the trends exhibited by the salt concentration dependence of diffusivities and the coordination of the cations with anions and with the polymer backbone remain qualitatively similar to those observed in non-crosslinked membranes. *Published by AIP Publishing.* https://doi.org/10.1063/1.5057708

I. INTRODUCTION

Recently, significant interest has centered on sulfonated copolymers as candidate membrane materials for desalination technologies.[1–5] Controlling the transport properties of water and ions in such desalination membranes is essential for these technologies to achieve better efficiency. Not surprisingly, a number of different physicochemical parameters, such as the architecture of chains, the chemistry of the polymer, etc., have been studied as means to control the solubility and mobility of water and ions. However, in almost all cases, cross-linking of the polymers is employed to achieve the requisite mechanical strength for membrane applications.[6,7] Typically, cross-linking reduces the swelling of the membrane,[8–10] but also influences the diffusion characteristics of the solvent and the salt.[11–13] Despite the ubiquity of cross-linking in the state-of-the-art materials,[7,10,14] there has been a dearth of theoretical and simulation studies on the influence of cross-linking on the transport properties of such polyelectrolyte membranes.

Some earlier experimental studies[6,7,15–17] have probed the influence of the degree of cross-linking on the properties of such desalination membranes. For instance, Jadwin *et al.*[15] have shown that cross-linking poly(hydroxyethyl methacrylate) (HEMA), using trimethylol propane trimethacrylate (TPT), results in a change of water/salt diffusivity selectivity of the material. Sundell *et al.*[16] have experimentally examined the impact of cross-linking on the transport characteristics of salt/water in disulfonated poly(arylene ether sulfone) copolymer membranes. They found that cross-linking effectively reduced the swelling of the polymer membranes and controlled the salt rejection.

The present work is a follow-up to our recent studies which were motivated by the experimental work by Kamcev *et al.*,[18] who extracted the individual diffusivities of salt ions in the crosslinked fixed charge membranes of CR61 polymers [as shown in Fig. 1(b)] as a function of the external salt NaCl concentration. They found that the transport properties of salt ions and water exhibit an intriguing dependence on salt concentration that is opposite to that seen in electrolyte solutions. Using atomistic molecular dynamics simulations, we recently[19] have probed diffusivities of salt ions and water as a function of the salt concentration in *non-crosslinked* membranes. Similar to experimental observations, we found a reversal in the trends relative to aqueous electrolytes of the Na^+ and Cl^- ions and water mobility with respect to the salt concentration. We have demonstrated that such salt concentration dependence of the mobilities' results arose from the fractions of free and condensed (near the polymer backbone) ions, the water structure, and ion pairing tendencies.

While our above-referenced study unearthed mechanisms pertinent to *non-crosslinked* membrane systems, it still left open the question of how applicable such concepts were to *crosslinked* polymer membranes which are often used in experiments (including the one which motivated our studies). While studies have focused on crosslinked polymers, their properties, and the development of efficient computational schemes to model and simulate such systems,[20–23] to our knowledge, there has not been any comparison of the structure and transport properties of non-crosslinked and crosslinked charged polymer membranes. Motivated by such considerations, in this study, we set out to answer the following questions: (a) What are the mechanisms underlying the transport of

a)Author to whom correspondence should be addressed: venkat@che.utexas.edu

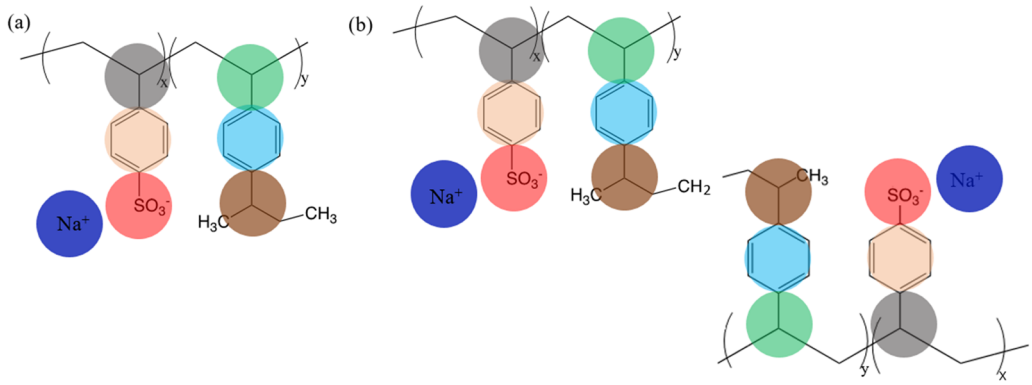

FIG. 1. Chemical structure of sulfonate polystyrene-*co*-divinylbenzene with corresponding DPD model for (a) non-crosslinked and (b) crosslinked polymers.

salt and water in *crosslinked*, charged polyelectrolyte membranes? (b) How are the structural and dynamical characteristics of salt and water influence the degree of cross-linking of polymers?

Unfortunately, atomistic simulations of the properties of crosslinked polymer membranes are computationally expensive due to the slow dynamics of crosslinked polymers. To overcome such constraints, in this work, we adopt a coarse-grained, mesoscopic model to build the crosslinked structure of the fixed charge polymer membranes in salt solutions of NaCl at different concentrations. We embed such a model within the dissipative particle dynamics (DPD) method,[24–31] which has proven to be an efficient simulation tool to study the structural and dynamical properties of polymer solutions and melts at long time and length scales. Using such a framework, we first obtain the diffusivities of salt/water in *non-crosslinked* polymer electrolyte membranes and demonstrate excellent agreement with the trends seen in our atomistic simulations. Subsequently, we study the influence of the degree of cross-linking of polymers on the diffusion characteristics of salts and water. We analyze the associated structural and dynamical characteristics to explain the mechanisms underlying our results.

The rest of the article is organized as follows: details of the simulation methodology and the different measures used to characterize the results are discussed in Sec. II. Results and discussion are presented in Sec. III where we first focus on the transport of salt/water in non-crosslinked membranes and compare the results obtained in mesoscale simulations with those seen in our atomistic model. Subsequently, we present the results quantifying the impact of the degree of cross-linking of the polymers on the transport properties of salt ions and water. We summarize our findings in Sec. IV.

II. MODEL AND METHODOLOGY

A. DPD simulations

For the mesoscale simulations, we employed a coarse-grained DPD framework[24,32] with the particles interacting via pairwise conservative soft repulsive nonbonded interactions, bonded Hookean forces, and electrostatic, random, and velocity dependent drag forces. The soft repulsion forces used are of the form

$$U\left(r_{ij}\right) = \begin{cases} \frac{a_{ij}(r-r_c)^2}{2r_c^2}, & r \leqslant r_c \\ 0, & r > r_c \end{cases}, \tag{1}$$

where r_c is the cut off radius and a_{ij} is the DPD interaction parameter between particles i and j. Following the standard approaches to DPD simulations,[24,32,33] the intra-component repulsion parameters a_{ii} between beads of the same type are set equal, whereas the repulsive parameters between different beads a_{ij} in Eq. (1) are computed from the following equation:

$$a_{ij} = \frac{\chi_{ij}}{0.286} + a_{ii}, \tag{2}$$

where χ_{ij} is the Flory-Huggins parameters between particles i and j. Repulsive parameters between different beads a_{ij} are presented in Table S1 in the supplementary material. As commonly used in DPD, the reduced density (ρr_c^3) and the friction coefficient (γ) of beads were set to 3 and 4.5, respectively, to maintain constant temperature at $k_BT = 1$.

The beads in the chains are connected by harmonic bonds $U(r_{ij}) = \frac{K_b}{2}(r_{ij} - r_0)^2$, where K_b is the bond constant and r_0 is the equilibrium bond length.[34] We also introduced the harmonic angle potentials $U\left(\theta_{ijk}\right) = \frac{K_\theta}{2}(\theta_{ijk} - \theta_0)^2$ between the beads of sulfonate groups of nearest neighbor bonds, where beads i and j are separated by bead k.[35]

The electrostatic interactions are modeled using the smeared charge approach with the Slater-type charge density distribution[33,35] $\rho(r) = \frac{q}{\pi(\lambda)^3}\exp(-\frac{2r}{\lambda})$, where λ is the effective smearing radius which is set to $0.25r_c$ for all charge beads. To account for long range electrostatic interactions, the standard Ewald summation[33] is used.

B. Coarse-grained model and parameters

The atomistic chemical structures of the non-crosslinked and crosslinked polymers, and the coarse-grained representations adopted in our study are depicted in Fig. 1. Explicitly, we divide the chemical units of the polymer into six types of DPD beads of comparable size. The mass of the phenyl ring bead was taken as a unit mass, and the masses of all other beads were scaled accordingly. Three water molecules ($N_w = 3$) were represented by one bead. To neutralize the charged sulfonate beads, one separate bead for a sodium ion as a counterion was used.

For non-crosslinked system, we considered randomly sulfonated polymers with 80 beads/chain with fixed charge fraction $f = 0.30$ with a total of 24 000 beads in a cubic simulation cell ~$20 \times 20 \times 20$ (r_c^3). The simulations were performed with five different concentrations of NaCl ranging from 0.04M to 1M. Salt Na^+ and Cl^- ions were represented by individual beads with charge distribution obtained from Refs. 34 and 36. The water volume fraction was fixed at 0.5 [which corresponds to 9 water molecules per sulfonate group (3 water beads per sulfonate group)] and was selected to match closely with the experimental study.[18] The bonded and non-bonded parameters for the DPD simulation of polymers, water, and salt ions were chosen from Refs. 26, 31, and 34–38, respectively.

All simulations were carried out using the DL_MESO DPD package.[39] Systems were run with the NVT simulations with periodic boundary conditions applied in all three dimensions. The equilibration was considered to be reached when the thermodynamic quantities such as the temperature and pressure of the systems, as well as the size and dimensions of polymer chains, exhibited no significant variation within the simulation time. Simulations were run further for 5×10^6 steps with 0.01 τ time step. Trajectories per 10 000 steps were saved for analysis. A snapshot of the systems after equilibration for 0.2M NaCl concentration in the non-crosslinked system is shown in Fig. S1 of the supplementary material.

C. Modeling crosslinked polymers

To model crosslinked polymer systems, we followed an approach similar to that proposed in Ref. 40. Explicitly, motivated by the experimental synthesis conditions,[18,41] the cross-link was based on attaching bonds between the beads of the side chain of the aliphatic carbons attached in the para position of the phenyl rings in hydrophobic blocks as shown in Fig. 1(b). For cross-linking simulations, the cross-link formation criterion is carried out after the equilibration portion of the non-crosslinked system. Beads were capable of cross-link formation if the distance between them falls within a pre-defined distance, $r_{cross} \ll r_c$. In a time step, if two crosslinkable beads were closer than r_{cross}, a (permanent) cross-link was formed by creating a bond (harmonic interaction) between those beads. Depending upon the density of cross-linking, we varied the degree of cross-linking to 25%, 35%, 50%, and 75%. We studied salt concentrations in the range 0.04–1M, which is similar to the regime explored in the experimental studies.[18] The sulfonation fraction ($f = 0.30$) of the polymer was also chosen to match with the experimental study.[18]

D. Calculation of diffusion coefficients

We determined the diffusion coefficients, D, for individual salts ions and water from mean square displacement ($MSD = \langle r_i(t) - r_i(0)^2 \rangle$, where $r_i(t)$ denotes the position of species i at time t) using the Einstein relation as follows:

$$D = \frac{\langle r_i(t) - r_i(0)^2 \rangle}{6t}.$$

The respective Na^+ ions MSDs are shown in Fig. S2 of the supplementary material for the extremes of the lowest (0.04M) and highest (1.0M) salt concentrations. In most cases, we chose an intermediate region of time to fit to the linear dependence and obtain the diffusion coefficients.

III. RESULTS AND DISCUSSION

A. Comparison of mesoscopic simulations with atomistic simulations

We begin our discussion by presenting a comparison of the results for the diffusion coefficients of Na^+, Cl^- ions, and water in non-crosslinked polyelectrolyte membranes as a function of NaCl concentration and compare these with our earlier results based on molecular dynamics simulations with atomistic resolution.[19,42]

Figures 2(a) and 2(b) depict the results for the diffusion coefficients of Na^+ and Cl^- ions in the polymer membrane

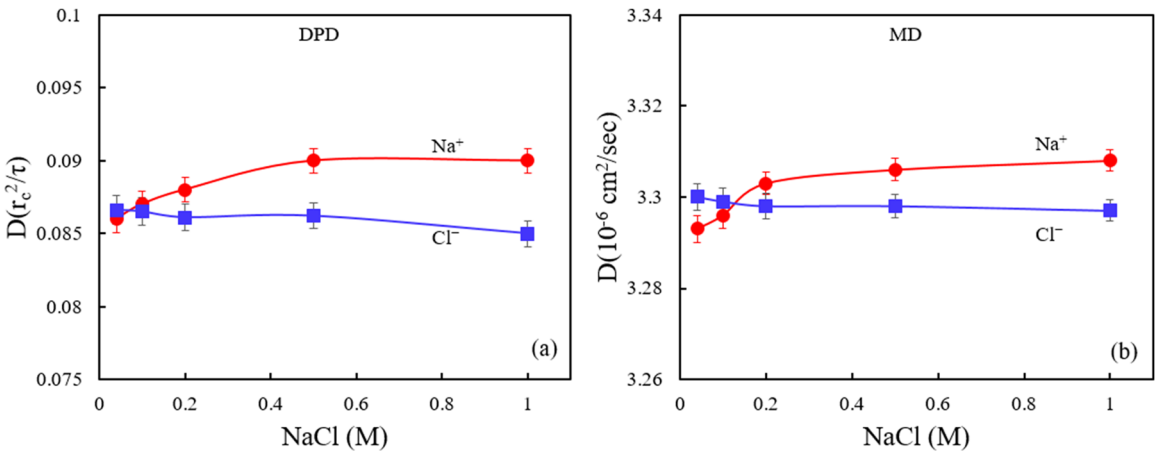

FIG. 2. Diffusion coefficient of Na^+ and Cl^- ions in membrane as a function of NaCl concentration using (a) DPD simulation method and (b) MD simulation results from Ref. 19. Reproduced with permission from Aryal and Ganesan, ACS Macro Lett. **7**, 739–744 (2018). Copyright 2018 American Chemical Society. The lines represent a guide to the eye.

from the mesoscale DPD approach [Fig. 2(a)] and the atomistic MD simulations [Fig. 2(b)], respectively, as a function of NaCl concentration. We observe that the results of diffusivity trends of Na^+ and Cl^- ions obtained using the mesoscale simulations are in good agreement with those reported in our earlier MD studies.[19] More specifically, we observe that the diffusivity of Na^+ increases with NaCl concentration, whereas the diffusivity of Cl^- is almost insensitive to NaCl concentration [Fig. 2(a)]. Moreover, in line with our earlier results, we also observe that the diffusivity of Na^+ ions in the membrane is higher than that of the Cl^- ions.

In our atomistic simulation studies,[19,42] we rationalized the above trends for the mobility of Na^+ and Cl^- ions by invoking the fractions of condensed (with the sulfonate groups of the polymer backbone), paired (associated cation-anions), and free ions and their respective mobilities. To effect a comparison with the atomistic simulations, we embarked on a similar structural classification in our mesoscale simulations. Na^+ ions were considered as "condensed" with sulfonate groups if they were within a cut off distance of 1.30 r_c [the location of the peak of the first coordination shell between S–Na^+ ions as shown in Fig. 7(a)]. The remaining Na^+ ions were further classified as either free or paired with Cl^- ions. The Cl^- ions were classified into three populations: (I) those which are associated with the condensed Na^+ ions; (II) those which are associated with free Na^+ ions; and (III) free Cl^- ions. We quantify the respective populations in terms of the fractions relative to the total number of ions of the respective species. Subsequent to identification (at $\tau = 0$) of condensed, paired, and free ions, their respective dynamics were used to characterize the diffusivities of the distinct populations of the ions.

Based on the above classification, similar trends are observed (Fig. 3) in atomistic and mesoscale simulations for the respective fractions and mobilities of the different categories of Na^+ and Cl^- ions. Explicitly, the fraction of condensed Na^+ ions decreases, while the fractions of paired and free ions increase with increasing NaCl concentration as shown in Fig. 3(a). Complementary to such results, Fig. 3(b) displays the individual mobilities of the condensed, paired, and free Na^+ ions in the membrane as a function of salt concentration. Therein, it can be seen that with an increase in the salt concentration, the diffusivity of free Na^+ ions monotonically increases, whereas the mobility of both the condensed and paired Na^+ ions remains relatively insensitive to the salt concentration. In the context of Cl^- ions, from the results displayed in Figs. 3(c)–3(d), we observe that the relative fraction (f) of the different populations satisfies the trend $f_I > f_{II} > f_{III}$ and the diffusivities of these populations follow the order $D_I < D_{II} < D_{III}$.

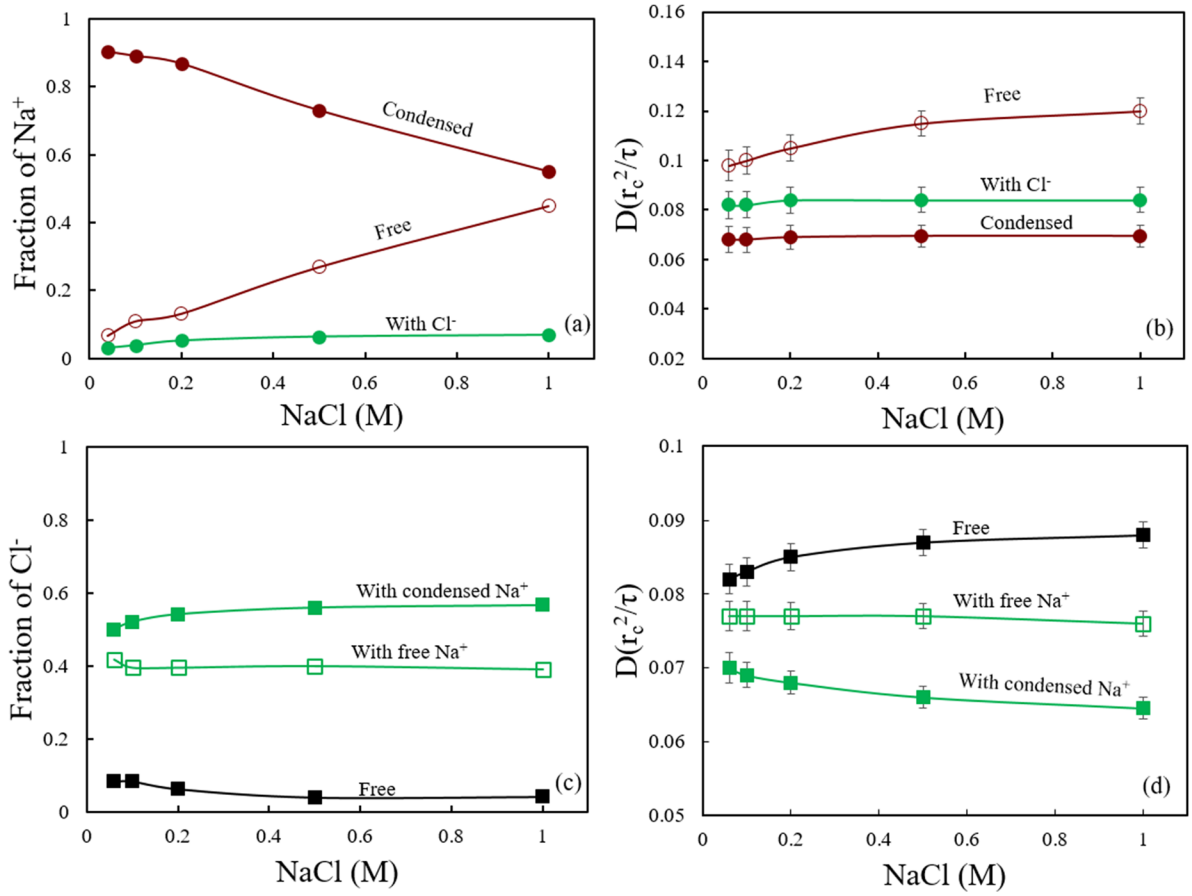

FIG. 3. Na^+ ions: (a) The fraction of Na^+ ions *condensed* with sulfonate groups, *paired with* Cl^- *ions*, and *free* ions. (b) Diffusivity of condensed, *paired with* Cl^-, and free Na^+ ions as a function NaCl concentration. Cl^- ions: (c) The fraction of Cl^- ions that are associated with condensed Na^+ ions, with free Na^+, and free Cl^- ions. (b) Diffusion coefficients of Cl^- ions that are associated with condensed Na^+ ions, with free Na^+, and free Cl^- as a function of NaCl concentration. The lines represent a guide to the eye.

Due to the correspondence between the results of the atomistic and the mesoscale simulations, the salt concentration dependence of the mobility of Na^+ ions can be explained similar to the results of our earlier work as a consequence of an increase in the free Na^+ ions which possess higher mobilities. The mobility of Cl^- ions can be understood to reflect an interplay of the mobilities of the free population and those associated with condensed Na^+ ions and is overall relatively insensitive to the salt concentrations.

We also compared the effect of salt concentration on the mobility of water in the polymer membrane [Fig. 4(a)] and observed similar trends between mesoscale and atomistic simulations. Explicitly, the diffusivity of water molecules is seen to increase with the salt concentration in the polymer membrane. Similar to the discussion presented in our earlier study, we rationalize our observations by invoking the influence of salt on the coordination of water and the internal structure. Explicitly, in our earlier work, it was argued that one of the factors influencing the water mobilities in the membrane relates to the relative fraction of water bound to the sulfonate beads. To characterize such a feature in the mesoscale simulations, we considered water as bound to the sulfonate beads if they were within a cut off distance of 1.5 r_c (first hydration shell from g(r) between S–O of water). The corresponding results displayed in Fig. 4(b) demonstrate that the fraction of free water increases with increasing salt concentrations. Since such a population of molecules possesses higher mobilities relative to the bound molecules, such results rationalize the increase in the diffusivity of water with increasing salt concentrations.

Overall, the results presented here serve to establish that the mesoscale simulations, despite their coarse-grained nature, reproduce most of the qualitative trends seen in our atomistic simulations relating to the mobilities and the structure of ions and water. With such a basis, we now seek to probe the influence of cross-linking on the structure and transport properties of the ions, water, and the polymer.

B. Influence of degree of cross-linking on structure and dynamics

In this section, we present results for the impact of the degree of cross-linking of polymers on the diffusivity of the polymer chains, the structure of the membrane, and the mobility of cations, anions, and water molecules in the polymer electrolyte membrane for a fixed salt concentration of 0.5M NaCl.

We begin this section by presenting the dynamical characteristics of the polymer chains and the internal structure of the membrane as a function of the degree of cross-linking. Figure 5(a) depicts the diffusion coefficient of the backbone beads of both blocks and sulfonated beads in the membrane (normalized by the diffusion coefficient of same beads in non-crosslinked polymers) as a function of the percentage of crosslinked chains. As we expect, the bead mobilities significantly reduce with increasing cross-linking densities. These results demonstrate that despite the coarse-grained nature of the model, our simulations do capture the dynamical features expected for crosslinked polymeric systems.

What is the influence of the degree of cross-linking on the internal structure of the polymer membrane? To address this question, we calculated the ionic cluster distribution as a function of the percentage of cross-linking of chains as shown in Fig. 5(b). For this purpose, we classified two sulfur beads of sulfonated groups to be in the same cluster if they were separated by less than 1.25 r_c [first hydration shell from g(r) between S–S as shown in Fig. S3 of the supplementary material]. We observe that with increasing cross-linking, there is a shift towards the formation of larger clusters at the expense of smaller clusters, which reflects [inset of Fig. 5(b)] as an increase in the average cluster size with increasing degree of cross-linking of polymer chains. Such trends can be rationalized by noting that that the cross-linking of the polymer beads brings the backbones of different polymer chains and, as a result, the sulfonate groups to closer proximity. As a

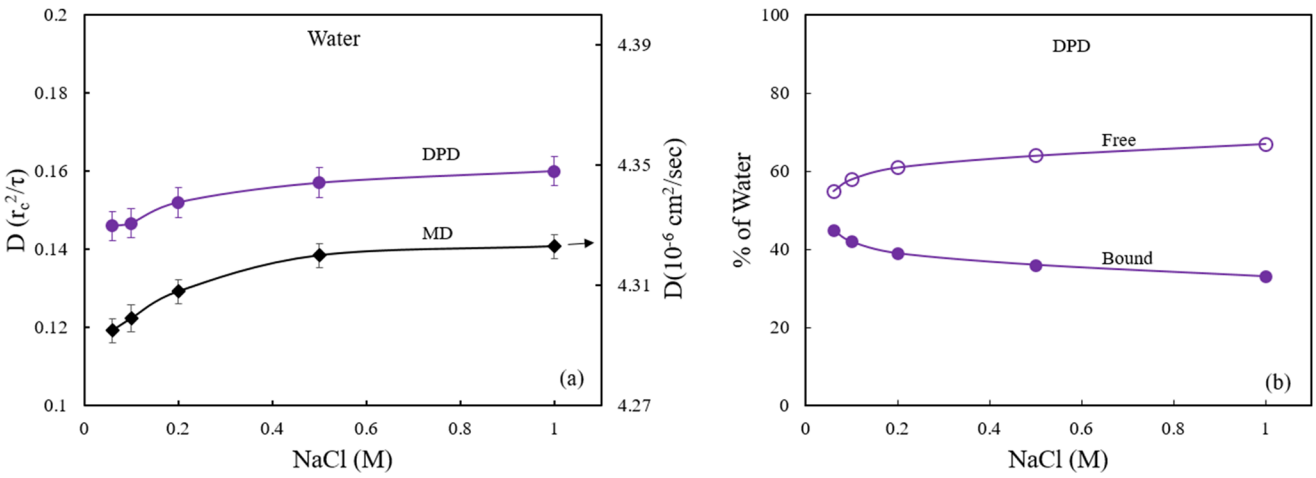

FIG. 4. (a) Diffusivity of water in the membrane from DPD simulation (left axis) and from MD simulation results (right axis, Ref. 19) as a function of NaCl concentration. (b) DPD simulation results for percentage of free and bound water as a function of NaCl concentration. The lines represent a guide to the eye.

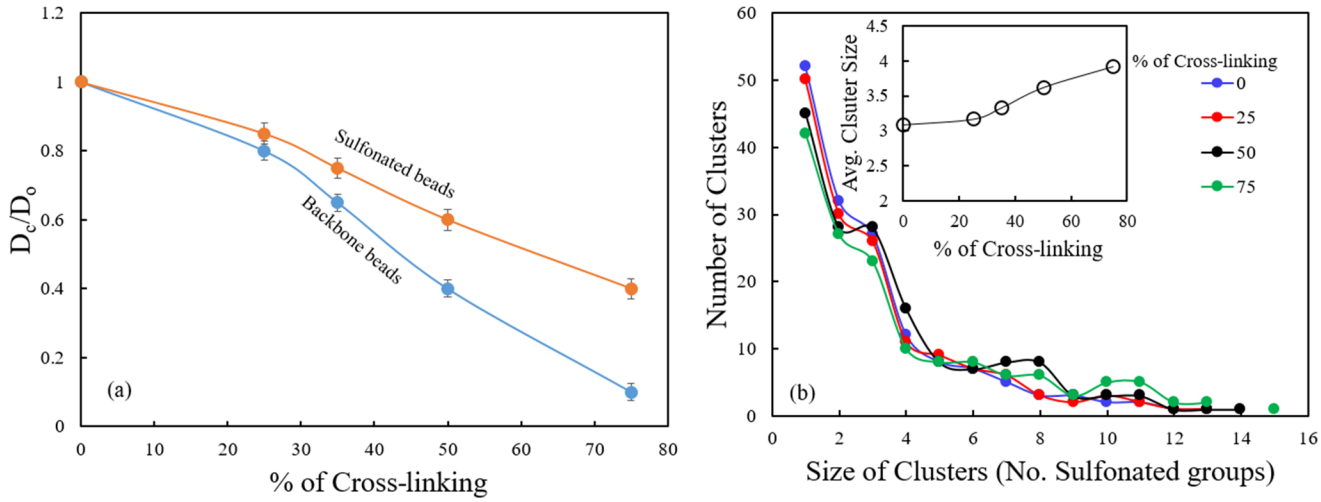

FIG. 5. (a) Normalized diffusion coefficients of polymer backbone beads (blue) and sulfonated beads (orange) and (b) cluster distribution of sulfonated beads as a function of the percentage of cross-linking of chains in the membrane at 0.5M salt concentration. Inset in (b) displays the average cluster size of the sulfonated beads as a function of the percentage of cross-linking. D_o = diffusion coefficient from un-crosslinked membranes and D_c = diffusion coefficient from crosslinked membranes. The lines represent a guide to the eye.

consequence, the sulfonate groups are expected to be in closer proximity in crosslinked membranes, leading to the larger cluster sizes as observed in our simulations.

In Fig. 6, we display the diffusion coefficients of Na^+ and Cl^- ions (normalized relative to non-crosslinked systems) as a function of the fraction of cross-linking. We observe that the mobilities of both Na^+ and Cl^- ions become reduced with increasing the degree of cross-linking of the polymers. More pertinently, we observe that the trend observed in non-crosslinked systems is preserved, and that even for crosslinked systems, the mobility of Na^+ ions in crosslinked membranes are higher than those of Cl^- ions.

The influence of cross-linking on ion dynamics can potentially arise from two distinct sources. One source of such results arises from the retardation of the polymer dynamics [Fig. 5(a)] arising from cross-linking of the chains. Since a fraction of the Na^+ ions are expected to be associated with the sulfonate groups in the polymer backbone, a retardation of the dynamics of the polymer backbone is expected to lead to a corresponding reduction in the mobility of such condensed ions. A

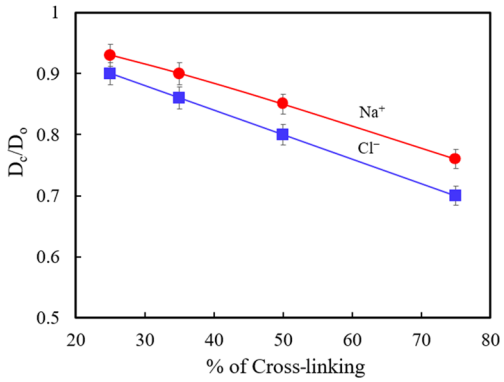

FIG. 6. Normalized diffusion coefficients of Na^+ and Cl^- ions as a function of percentage of cross-linking of chains in membrane at 0.5M salt concentration. The lines represent a guide to the eye.

second source of the influence of cross-linking arises from the potential impact of cross-linking on the association characteristics between the Na^+ ions and the sulfonate groups. Indeed, as observed in the results of Fig. 5(b), the introduction of cross-links modifies the distribution of sulfonate groups. In turn, such changes may influence the distribution and the fraction of Na^+ ions condensed with the sulfonate groups.

To identify the specific influence of above features, we characterized the influence of cross-linking on the radial distribution function between S–Na^+. The results for radial distribution functions [Fig. 7(a)] indicate that the association between the Na^+ ions and the sulfur atoms become stronger with increasing degree of cross-linking. We quantified such results further by delineating the Na^+ ions into fractions of condensed and free ions. Explicitly, we categorized the Na^+ ions as condensed if they were within a cutoff distance of 1.28 r_c [the location of the peak of first coordination shell from Fig. 7(a)] of the sulfur atoms. Ions which were beyond that distance were categorized as free. From the result displayed in Fig. 7(b), we observe that the fraction of the condensed Na^+ ions increases with increasing degree of crosslinked polymers. Such results demonstrate that cross-linking of the polymers in the membrane does exert an influence on the structural characteristics and the association behavior between the cations and the charged polymer backbone. Since such condensed ions are expected to possess lower mobilities than the free ions, such results contribute to the overall reduction in the diffusivity of Na^+ ions with increasing degree of cross-linking.

Figures 7(c) and 7(d) quantify the dynamical effects of cross-linking by displaying the mobilities of the *condensed* ions in two representations: the diffusivities relative to the case of non-crosslinked systems and the diffusivities normalized by the corresponding mobilities of the sulfonate beads. As expected, the diffusivities of the condensed ions decrease with increasing degree of cross-linking. More interestingly, from Fig. 7(d), we observe that in a normalized representation,

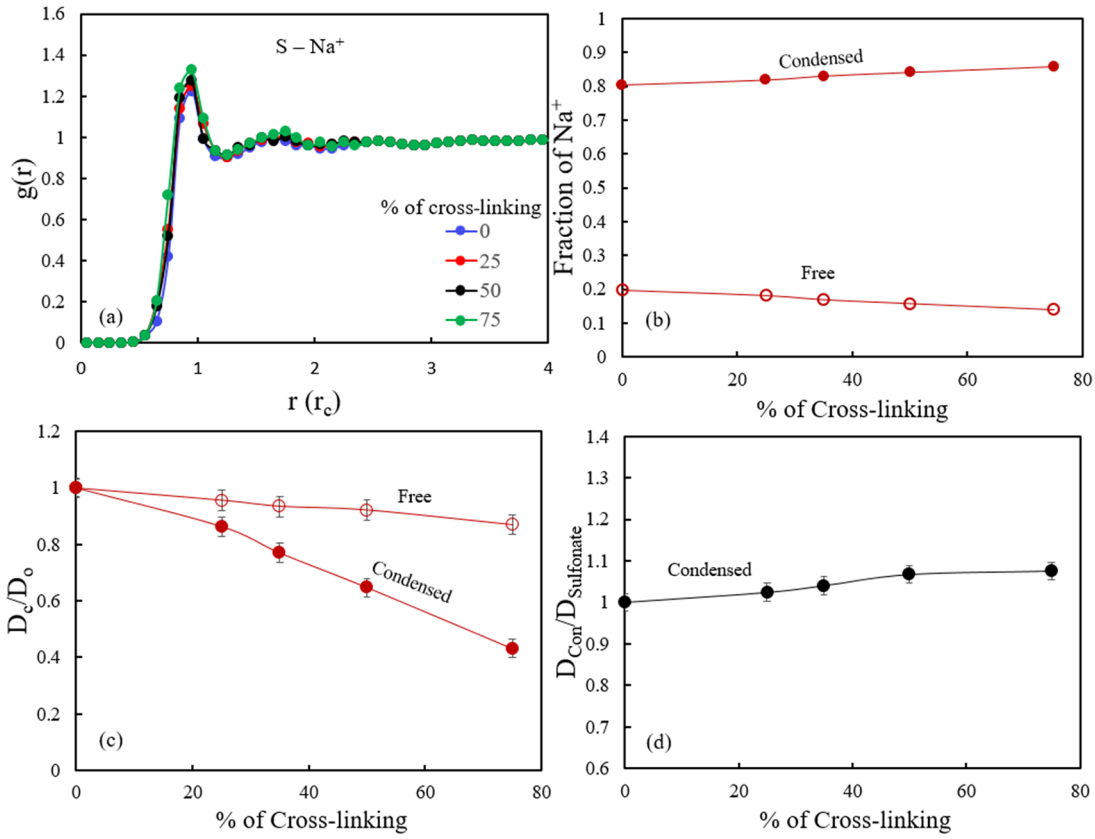

FIG. 7. (a) Radial distribution function of S–Na^+, (b) the fractions of Na^+ ions condensed with sulfonated beads and free ions, (c) normalized diffusion coefficients of condensed and free Na^+ ions, and (d) divided diffusion coefficient of condensed Na^+ [from (c)] by diffusion coefficient of sulfonated groups [from Fig. 5(a)] as a function of the percentage of cross-linking of chains in membrane at 0.5M NaCl salt concentration. The lines represent a guide to the eye.

the mobility of the condensed Na^+ ions remains practically a constant indicating that the dynamical effects manifesting in the mobility of *condensed* Na^+ ions arise as a consequence of the slowing of the sulfonate groups as a result of cross-linking.

To rationalize the influence of cross-links on the mobility of Cl^- ions, we observe that the population of Cl^- ions associated with the condensed Na^+ ions increases with increasing degree of cross-linking [Fig. 8(a)]. Such results can be understood as a consequence of the increased fraction of the *condensed* Na^+ ions. The dynamics of such associated Cl^- ions are in general expected to be slower than the free Cl^- ions. Moreover, the cross-link-induced slowing of the condensed Na^+ ions discussed in the context of the results of Fig. 7 is also expected to contribute as an additional source of hindered mobilities of the associated Cl^- ions. Such expectations are confirmed in the results displayed in Fig. 8(b), wherein it is seen that the mobility of the Cl^- ions associated with Na^+ ions

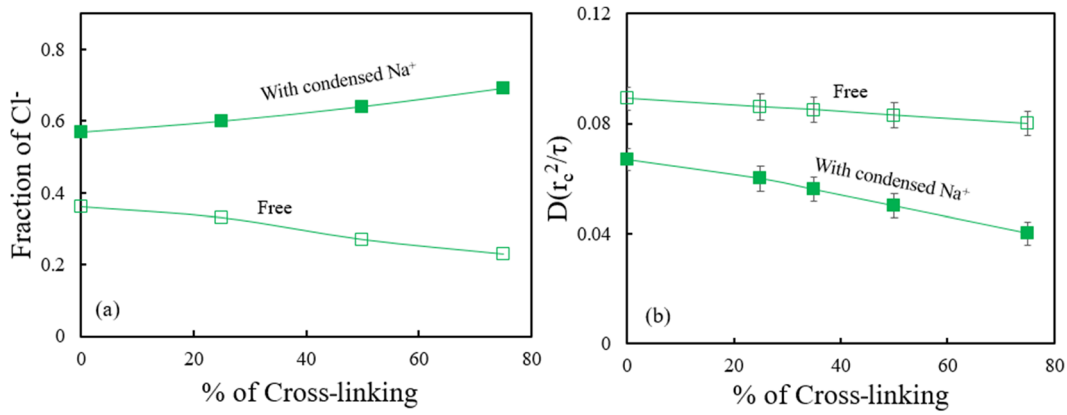

FIG. 8. (a) The fractions of Cl^- condensed with Na^+ ions and free ions and (b) Diffusivity of of Cl^- condensed with Na^+ ions and free ions as a function of the percentage of cross-linking polymers in membrane at 0.5M NaCl salt concentration. The lines represent a guide to the eye.

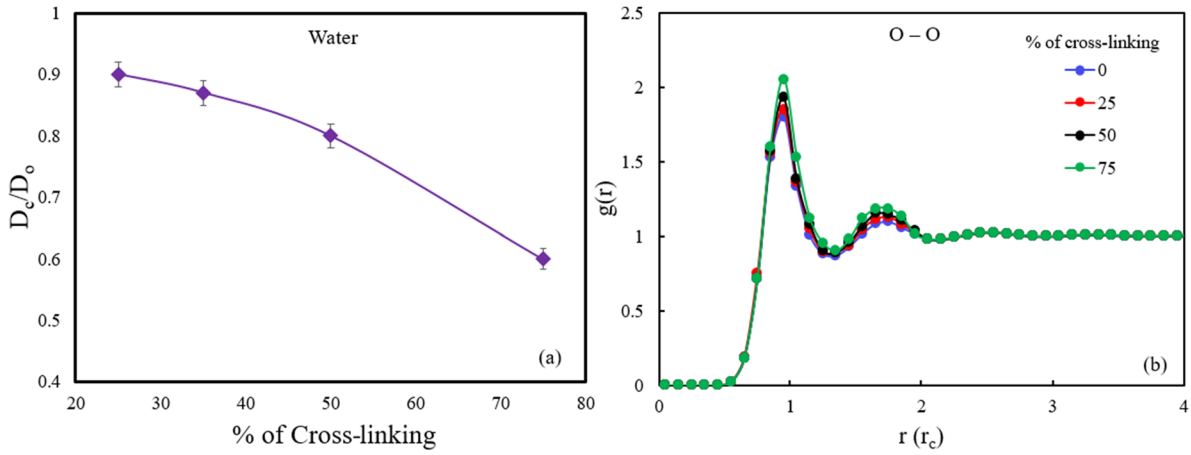

FIG. 9. (a) Normalized diffusivity of water, and (b) radial distribution function of water-water beads of as a function of the percentage of cross-linking of polymers in membrane at 0.5M salt concentration. The lines represent a guide to the eye.

do indeed decrease with increasing degree of cross-linking. Together, the increase in the fraction of the associated Cl^- ions and the decrease in their mobilities rationalize the influence of cross-links shown in Fig. 6.

Next, we present results for the influence of cross-linking of polymer chains on the diffusivity of water molecules [Fig. 9(a)]. Similar to the trends seen for the salt ions, the mobility of water molecules is seen to become reduced with increasing degree of cross-linking.

In our previous work, we ascribed that the salt concentration induced changes in water mobilities to the fraction of the water molecules "bound" to the backbone sulfonate groups. Such characteristics were in turn shown to be correlated to the size of the water clusters in the membrane. More specifically, the presence of larger water clusters and the higher fraction of bound water molecules led to lower mobilities for the water molecules.

In the present context, we expect a part of the influence of the cross-linking on water mobilities to arise from the slowing of the polymer molecules themselves. To probe if there are further structural effects arising from the cross-linking of polymers, we probed the coordination of water and the internal structure by calculating the radial distribution function g(r) between water beads as a function of the degree of cross-linking [Fig. 9(b)]. With increasing percentage of cross-linking the polymer chains, the intensities of both peaks in the radial distribution function slightly increase, which suggests that the structural characteristics of water intensify with increasing degree of cross-linking.

We also performed an analysis of the water clusters as a function of the degree of cross-linking. For this purpose, we classified two oxygen atoms of water to be in the same cluster if they are separated by less than 1.33 r_c [first hydration shell from g(r) between O–O of water as shown in Fig. 9(b)]. From the result displayed in Fig. 10(a), we observe that the average water cluster size increases with increasing degree of cross-linking. Similar to the results presented in our earlier articles, such increases are seen to manifest in the increased fraction of water molecules bound to the ionic groups, as shown in Fig. 10(b).

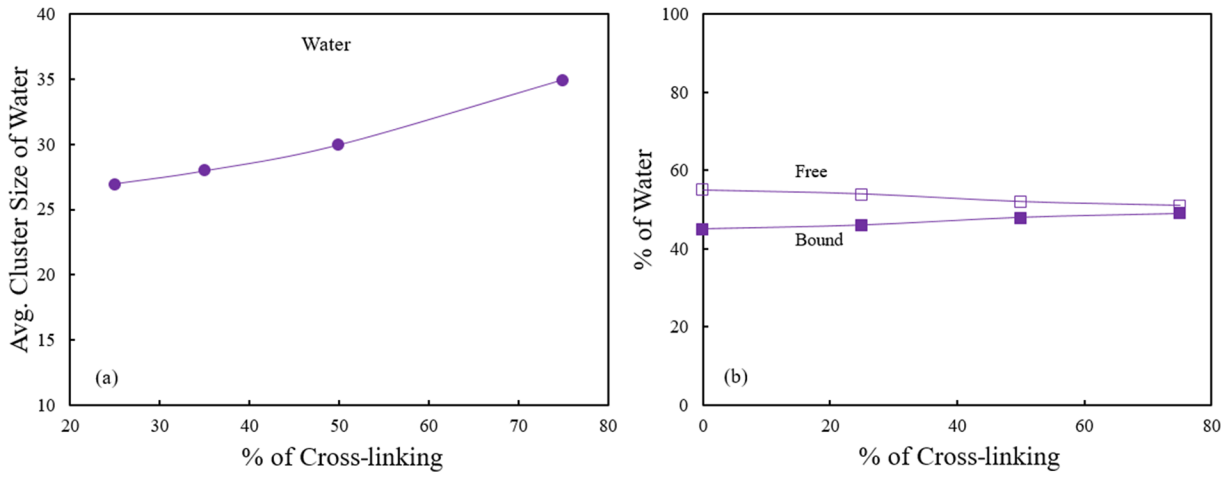

FIG. 10. (a) The average cluster size of water and (b) the percentage of free and bound water in the membranes as a function of the percentage of cross-linking at 0.5M NaCl salt concentration. The lines represent a guide to the eye.

Together, the results of Figs. 9 and 10 suggest that the degree of cross-linking does influence the structural characteristics of water molecules and leads to an increased size of water clusters and an enhanced fraction of water bound to the ionic groups. In conjunction with the reduced mobility of the polymer membrane, such factors explain the reduced mobility of the water with increasing degree of cross-linking.

C. Comparison of crosslinked with non-crosslinked membranes as a function of salt concentration

In this section, we present a comparison of the results for the diffusion coefficients of Na^+, Cl^- ions, and water in crosslinked polyelectrolyte membranes as a function of NaCl concentration and compare these with the results of non-crosslinked membranes from this study (mesoscale DPD approach).

Figures 11(a) and 11(b) compare the salt concentration dependence of the diffusion coefficients of Na^+ and Cl^- ions in both the crosslinked polymer and non-crosslinked membranes [from Fig. 2(a)] as a function of the NaCl concentration. We observe that the results of diffusivity trends of both Na^+ and Cl^- ions in crosslinked systems are qualitatively similar to those seen in non-crosslinked systems. More specifically, similar to the results of non-crosslinked systems, we note that the diffusivity of Na^+ increases with NaCl concentration, whereas the diffusivity of Cl^- is almost insensitive to NaCl concentration [Fig. 11(a)]. Moreover, we also observe that the diffusivity of Na^+ ions in the membrane is higher than that of the Cl^- ions. These results are in qualitatively good agreement with the experiment results of Kamcev *et al.*[18] who extracted the individual diffusivities of salt ions in the crosslinked fixed charge membranes of CR61 polymers as a function of the external salt NaCl concentration.

To explain the origin of the above trends for the mobility of Na^+ and Cl^- ions, we classified the ions using similar approaches as we did for non-crosslinked systems (discussed in the context of Fig. 3) by invoking the fractions of the

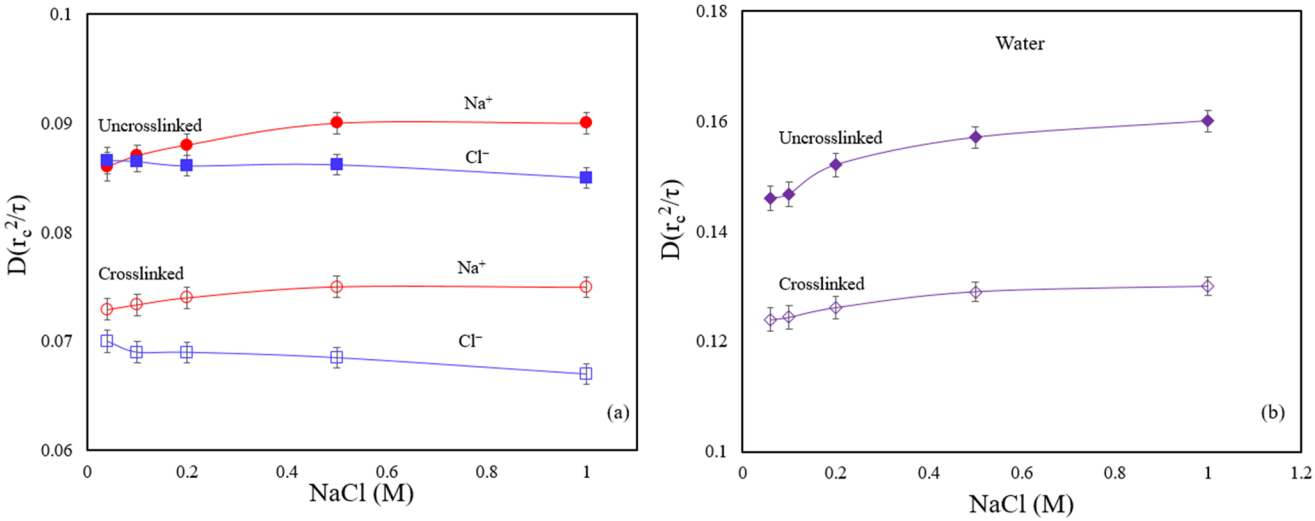

FIG. 11. (a) Diffusion coefficient of Na^+ and Cl^- ions and (b) diffusivity of water in non-crosslinked membrane (closed symbols) and in the crosslinked membrane (open symbols) as a function of NaCl concentration. The lines represent a guide to the eye.

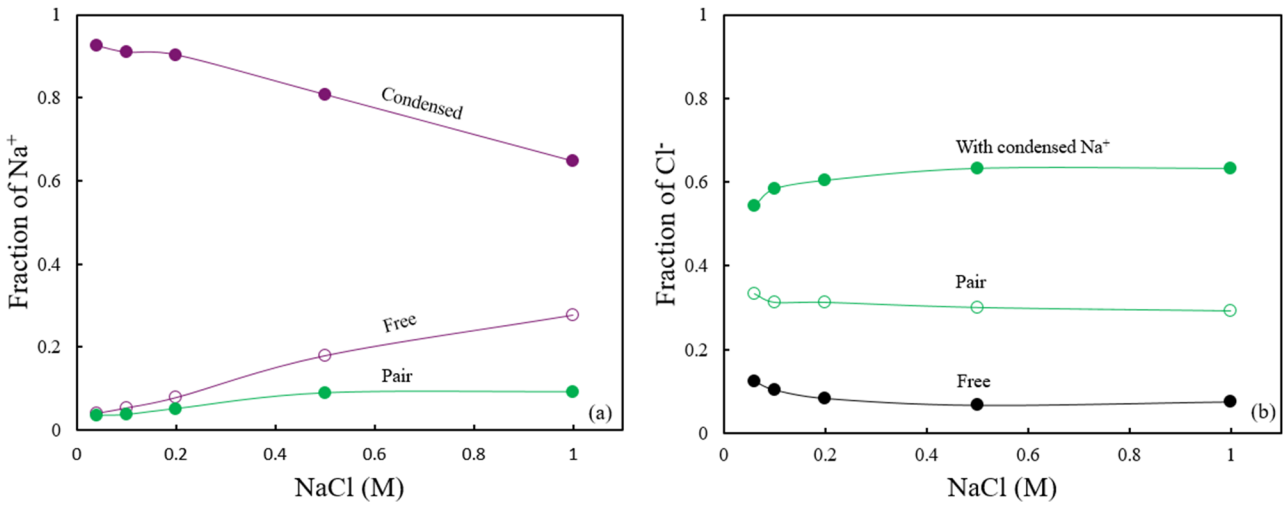

FIG. 12. In crosslinked membrane: (a) The fraction of Na^+ ions *condensed* with sulfonate groups, *paired with* Cl^- *ions*, and *free* ions. (b) The fraction of Cl^- ions that associated with condensed Na^+ ions, with free Na^+, and free Cl^- ions. The lines represent a guide to the eye.

condensed (with the sulfonate groups of the polymer backbone), paired (associated cation-anions), and free ions. From the results displayed in Fig. 12, we see qualitatively similar trends in both crosslinked and non-crosslinked systems for the respective fractions and mobilities of the different categories of Na^+ and Cl^- ions.[19] Explicitly, the fraction of condensed Na^+ ions decreases, while the fractions of paired and free ions increase with increasing NaCl concentration. In the context of Cl^- ions, the fraction of Cl^- ions associated with condensed Na^+ ions are seen to increase with increasing NaCl concentration.

The above results demonstrate that both the salt concentration dependencies and their mechanistic origins share similar features in crosslinked and non-crosslinked membranes. Explicitly, the increase in the fraction of free Na^+ ions and the higher mobility of such a population can be attributed as responsible for the mobility of Na^+ ions in the membrane to increase with increasing salt concentration, whereas the mobility of Cl^- ions is dominated by the population of condensed and paired ions and is relatively constant for all concentrations.

We also examined the effect of salt concentration on the mobility of water in the crosslinked polymer membrane [Fig. 10(b)] and observed a similar trend for the salt concentration dependencies as seen in non-crosslinked systems. Explicitly, the diffusivity of water molecules is seen to slightly increase with the salt concentration in the crosslinked polymer membrane. Similar to non-crosslinked systems, we observe that such results arise from the influence of the charged polymer membrane on the water structure and the population of free and bound water to sulfonate beads as shown (Fig. 13).

Overall, we observe that the trends exhibited by the salt concentration dependence of diffusivities, and the coordination of the cations with anions and with the polymer backbone exhibit striking similarities between crosslinked and non-crosslinked membranes. We hypothesize that since the polymer chains are crosslinked by the side chain of hydrophobic blocks which are phase separated from the hydrophilic blocks, the crosslinking only exerts a limited influence on the hydrophilic domains which support the transport of ions/water. As a consequence, beyond the dynamical effects on the polymer backbone, and some of the quantitative aspects of structural effects arising from the changes in the ionic cluster size distributions and the coordination behaviors discussed in Sec. III B, much of the physics arising in crosslinked membranes are seen to be captured in the simulations of non-crosslinked systems.

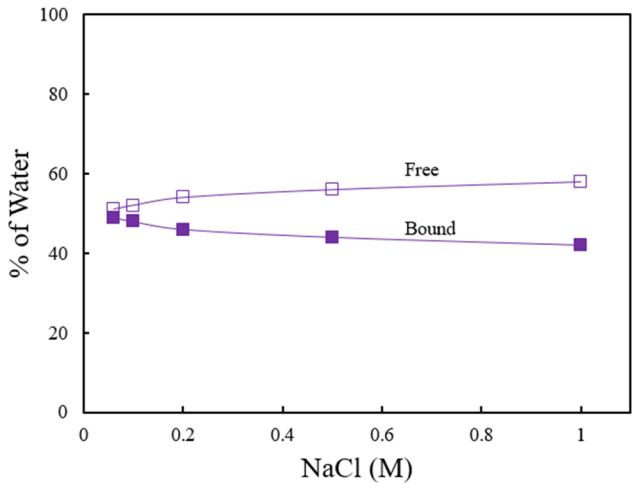

FIG. 13. In crosslinked membrane: Fraction of free and bound water as a function of NaCl concentration. The lines represent a guide to the eye.

IV. CONCLUSIONS

In this article, we presented the results from coarse-grained dissipative particle dynamics quantifying the influence of the degree of cross-linking of polymers on the structure and dynamics of water and salt ions in polyelectrolyte desalination membranes. In the first part of this study, the results for salt ion and water diffusivities (along with supporting structural characteristics) were probed as a function of the salt concentration in non-crosslinked polymer electrolyte membranes and compared to the trends reported in our earlier studies which used atomistic MD simulations.[19] Such comparisons demonstrated that the DPD simulations reproduced results in good agreement with our atomistic simulations studies and provided a basis for the use of mesoscale simulations for examining the influence of cross-linking on the structure and the transport of water and salt ions in such membranes.

In the second part of the article, we presented the results for the influence of the degree of cross-linking of polymer chains on the transport properties of salt/water in polyelectrolyte membranes. With increasing degree of cross-linking on polymer chains, the diffusivities of salt/water reduced significantly. Our analysis suggested that the structural changes resulting from cross-linking also influence such trends, in addition to the dynamical changes arising from the slower mobility of polymer chains. Interestingly, much of the salt concentration dependencies of the structural and dynamical characteristics exhibited trends similar to non-crosslinked membranes. Such results suggest that atomistic simulations of *non-crosslinked* membranes can serve as a useful means to probe the interplay between the chemistry and the transport properties of realistic and crosslinked polyelectrolyte membranes.

SUPPLEMENTARY MATERIAL

See supplementary material for the simulation snapshot, mean-squared displacements of ions, and the radial distribution function of S–S as a function of degree of cross-linking (see Figs. S1-S3, respectively).

ACKNOWLEDGMENTS

We thank Professor Benny Freeman and Dr. Jovan Kamcev for many useful discussions. We acknowledge funding in part by grants from the Robert A. Welch Foundation (Grant No. F1599) and the National Science Foundation (Grant No. DMR-1721512), and the King Abdullah University of Science and Technology (Grant No. OSR-2016-CRG5-2993-1) which helped support the development of atomistic simulations and the results arising from such a framework. The simulations

work involving DPD simulations was supported as part of the Center for Materials for Water and Energy Systems, an Energy Frontier Research Center funded by the U.S. Department of Energy, Office of Science, Basic Energy Sciences under Award No. DE-SC0019272. The authors acknowledge the Texas Advanced Computing Center (TACC) for computing resources.

[1]M. A. Hickner, Mater. Today **13**, 34 (2010).
[2]G. M. Geise, H. S. Lee, D. J. Miller, B. D. Freeman, J. E. McGrath, and D. R. Paul, J. Polym. Sci., Part B: Polym. Phys. **48**, 1685 (2010).
[3]J. Grimm, D. Bessarabov, and R. Sanderson, Desalination **115**, 285 (1998).
[4]M. Turek and B. Bandura, Desalination **205**, 67 (2007).
[5]K. P. Lee, T. C. Arnot, and D. Mattia, J. Membr. Sci. **370**, 1 (2011).
[6]G. E. Zaikov, A. P. Iordanskii, and V. S. Markin, *Diffusion of Electrolytes in Polymers* (VSP, Utrecht, The Netherlands, 1988).
[7]Y.-S. Ye, J. Rick, and B.-J. Hwang, Polymers **4**, 913 (2012).
[8]S. K. Bajpai and S. Singh, React. Funct. Polym. **66**, 431 (2006).
[9]P. J. Flory and J. Rehner, J. Chem. Phys. **11**, 521 (1943).
[10]G. M. Geise, D. R. Paul, and B. D. Freeman, Prog. Polym. Sci. **39**, 1 (2014).
[11]A. C. Sagle, H. Ju, B. D. Freeman, and M. M. Sharma, Polymer **50**, 756 (2009).
[12]H. Ju, B. D. McCloskey, A. C. Sagle, Y. H. Wu, V. A. Kusuma, and B. D. Freeman, J. Membr. Sci. **307**, 260 (2008).
[13]G. M. Geise, H. B. Park, A. C. Sagle, B. D. Freeman, and J. E. McGrath, J. Membr. Sci. **369**, 130 (2011).
[14]H. Ju, A. C. Sagle, B. D. Freeman, J. I. Mardel, and A. J. Hill, J. Membr. Sci. **358**, 131 (2010).
[15]T. A. Jadwin, A. S. Hoffman, and W. R. Vieth, J. Appl. Polym. Sci. **14**, 1339 (1970).
[16]B. J. Sundell, E. S. Jang, J. R. Cook, B. D. Freeman, J. S. Riffle, and J. E. McGrath, Ind. Eng. Chem. Res. **55**, 1419 (2016).
[17]H. Yasuda, A. Peterlin, C. K. Colton, K. A. Smith, and E. W. Merrill, Makromol. Chem. **126**, 177 (1969).
[18]J. Kamcev, D. R. Paul, G. S. Manning, and B. D. Freeman, Macromolecules **51**, 5519 (2018).
[19]D. Aryal and V. Ganesan, ACS Macro Lett. **7**, 739–744 (2018).
[20]Y. Wu, S. Joseph, and N. R. Aluru, J. Phys. Chem. B **113**, 3512 (2009).
[21]E. Chiessi, F. Cavalieri, and G. Paradossi, J. Phys. Chem. B **111**, 2820 (2007).
[22]J. Mijović and H. Zhang, J. Phys. Chem. B **108**, 2557 (2004).
[23]S. S. Jang, W. A. Goddard, M. Yashar, and S. Kalani, J. Phys. Chem. B **111**, 1729 (2007).
[24]R. D. Groot and P. B. Warren, J. Chem. Phys. **107**, 4423 (1997).
[25]P. Español and P. B. Warren, J. Chem. Phys. **146**, 150901 (2017).
[26]C. Wang and S. J. Paddison, Soft Matter **10**, 819 (2014).
[27]H. Liu, S. Cavaliere, D. J. Jones, J. Rozière, and S. J. Paddison, J. Phys. Chem. C **122**, 13130 (2018).
[28]S. Liu, J. Savage, and G. A. Voth, J. Phys. Chem. C **119**, 1753 (2015).
[29]R. Jorn and G. A. Voth, J. Phys. Chem. C **116**, 10476 (2012).
[30]C. Hu, T. Lu, and H. Guo, J. Membr. Sci. **564**, 146 (2018).
[31]J. T. Wescott, Y. Qi, L. Subramanian, and T. Weston Capehart, J. Chem. Phys. **124**, 134702 (2006).
[32]A. Maiti and S. McGrother, J. Chem. Phys. **120**, 1594 (2004).
[33]M. González-Melchor, E. Mayoral, M. E. Velázquez, and J. Alejandre, J. Chem. Phys. **125**, 224107 (2006).
[34]M. T. Lee, A. Vishnyakov, and A. V. Neimark, J. Chem. Theory Comput. **11**, 4395 (2015).
[35]M. T. Lee, A. Vishnyakov, and A. V. Neimark, J. Chem. Phys. **144**, 014902 (2016).
[36]E. Mayoral and E. Nahmad-Achar, J. Chem. Phys. **137**, 194701 (2012).
[37]A. Vishnyakov, R. Mao, M. T. Lee, and A. V. Neimark, J. Chem. Phys. **148**, 024108 (2018).
[38]E. Mayoral and A. G. Goicochea, J. Chem. Phys. **138**, 094703 (2013).
[39]M. A. Seaton, R. L. Anderson, S. Metz, and W. Smith, Mol. Simul. **39**, 796 (2013).
[40]G. Kacar, E. A. J. F. Peters, and G. de With, Soft Matter **9**, 5785 (2013).
[41]J. Kamcev and B. D. Freeman, Annu. Rev. Chem. Biomol. Eng. **7**, 111 (2016).
[42]D. Aryal and V. Ganesan, J. Phys. Chem. B **122**, 8098 (2018).